

## Polarization measurements of thermally-sensitised advanced gas reactor (AGR) fuel cladding in trace electrolytes

C.H. Phuah<sup>1</sup>, M.P. Ryan<sup>1</sup>, P. Standing<sup>2</sup> and W.E. Lee<sup>1</sup>

<sup>1</sup>Department of Materials, Imperial College London

<sup>2</sup>Thorp Technical Department, Sellafield Limited, Seascale, Cumbria

(correspondence: m.p.ryan@imperial.ac.uk)

### ABSTRACT

Interim storage of the Advanced Gas Reactor's (AGR) spent fuel in a demineralised-water cooling pond, which contains trace amounts of chloride albeit under strict environmental control, poses a corrosion concern over time. Sensitization is a condition characterized by grain boundary chromium depletion to certain depths and widths and is caused by radiation-induced segregation (RIS), elevated temperature exposure and spallation mechanisms. The presence of sensitized regions in the fuel cladding increases the corrosion risk in this material. This work aims to establish the level of sensitization at which the AGR fuel cladding, made of austenitic stainless steel 20Cr/25Ni/Nb, becomes susceptible to corrosion in an aqueous environment with trace concentrations of chloride. Energy Dispersive X-ray (EDX) analysis on a thin foil cross-section of a 400°C 96hour heat-treated AGR fuel cladding, obtained using the focused ion beam instrument, measured a 34.2 %, 36.2 % and 36.3 % reduction in grain boundary Cr, Fe and Ni, respectively. This degree of sensitisation – a 36.2 at% decrease in Cr – exhibits corrosion at a potential of ~1.0 V (Ag|AgCl) in 0.01M NaCl whereas the as-received cladding, does not exhibit corrosion up to the oxygen evolution region.

### BACKGROUND

AGR fuel claddings are hollow tubes made of austenitic stainless steel 20Cr/25Ni/Nb 1 m long, 7.24 mm in radius and with 0.38 mm wall thickness<sup>2</sup>. Figure 1 shows a fuel cladding, which also has circumferential ribs of 0.31 mm at every 2.5 mm pitch to improve heat transfer, used to encapsulate the fuel pellets so that they remain leak-free in the reactor core operating at a 40 bar pressure of CO<sub>2</sub>-coolant circulation. The employed cladding has enhanced creep resistance through homogeneously dispersed fine Nb(C,N) particles in the matrix and oxidation resistance through the spontaneously developed Cr<sub>2</sub>O<sub>3</sub> surface film. However, irradiation and high temperature exposure over a critical service period change the matrices composition considerably and as a result adversely impact on other endurance properties which include embrittlement, void swelling and stress corrosion cracking. Corrosion processes, in particular, have profound association with sensitisation – a type of microstructural defect characterized by grain boundary chromium depletion to certain widths and depths – in which a metal sensitised to below the 11%wt-chromium threshold level is not able to repassivate with Cr<sub>2</sub>O<sub>3</sub> and becomes prone to intergranular stress corrosion cracking<sup>3-7</sup>.

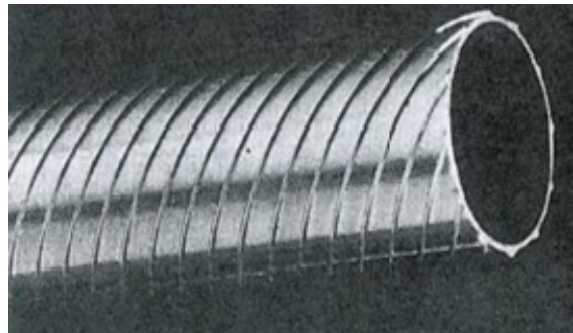


Figure 1 AGR fuel cladding made of alloy 20Cr/25Ni/Nb

That sensitisation occurs principally through radiation-induced segregation (RIS), elevated temperature exposure, and spallation routes is well established<sup>1,6,8,9</sup>. RIS is a point defect-solute interaction which results in compositional evolution to the cladding's 20Cr/25Ni matrix, notably solute segregation at the grain boundaries<sup>6</sup>. Figure 2 shows measurements of solute segregation at a grain boundary of a post-irradiated AGR fuel cladding where substantial degree of sensitisation is observed – Cr is depleted from 20%wt to less than 5%wt – alongside Fe which is also depleted in contrast to Ni and Si which are enriched<sup>1</sup>.

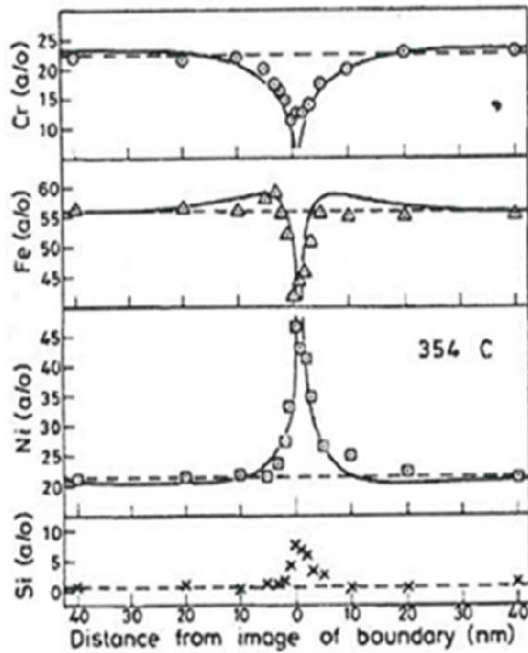


Figure 2 Radiation-induced segregation

Elevated temperature exposure, hand-in-hand, encourages sensitisation through precipitation of chromium-rich carbides ( $M_{23}C_6$ ) leaving the adjacent grain boundaries chromium depleted<sup>8</sup>. At certain temperatures  $M_{23}C_6$  precipitates are predominantly formed at the expense of Nb(C,N) – according to the time-temperature-precipitation diagram for AGR fuel cladding shown in Figure 3 – which suggests that the metal’s susceptibility is inherently variable along the fuel pin and between fuel pins which experience gradients in temperature and neutron fluxes due to coolant circulation and repeated thermal cycling (adjustments to power conditions)<sup>9</sup>. Spallation, the third cause of sensitisation, is a condition characterized by rupture of the surface  $Cr_2O_3$  particles, encouraged by the turbulence of  $CO_2$ -coolant circulation, as a result of interfacial stress that arise from swelling of the fuel pellets and differences in contraction rates between the metal cladding and the  $Cr_2O_3$  particle itself<sup>10-12</sup>. Consequently, regeneration of the spalled  $Cr_2O_3$  drives the migration of the bulk chromium to the surface thereby inducing chromium depletion. In fact, spallation also results in severe surface irregularities where pits up to  $40\mu m$  deep (about 10% of the 0.38mm wall thickness) have been measured and they may potentially become sites for accommodation of corrosive agents for corrosion initiation<sup>2</sup>.

Corrosive agents that participate in corrosion processes include e.g. anion chloride<sup>13, 14</sup>. Figure 4 illustrates a pit in which chloride is potentially located and subsequently engaged in oxidation reactions ( $M(s) \rightarrow M^{n+} + ne$ ) that lead to metal dissolution; the electrons are conveniently dissipated at the environment through cathodic reactions ( $O_2 + 2H_2O + 4e \rightarrow 4OH^-$ ) but the cation  $M^{n+}$

attracts more free chloride ( $Cl^-$ ) into the pit to maintain charge neutrality by forming metal-chloride complexes ( $M^+Cl^-$ ). The latter constituent, however, is metastable, can hydrolyze water ( $M^+Cl^- + H_2O \rightarrow MOH + H^+ + Cl^-$ ) and creates an acidic ( $H^+$ ) environment in the pit which promotes a self-sustaining interaction with excess chloride in the solution. Propagation beyond the pits is likely because a sensitised metal does not have adequate chromium for repassivation through chromia, leading to stress corrosion cracking and ultimately exposing the fuel pellets to the environment.

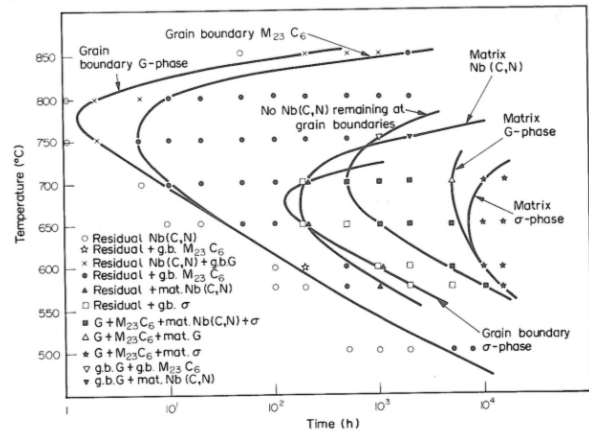


Figure 3 Precipitation characteristics of the AGR fuel cladding<sup>2</sup>

Quantification of a metal’s potential for corrosion is usually provided by electrochemical techniques, among others the commonly employed anodic polarization method<sup>13-16</sup>. In this method, the current density of the material of interest is measured as a function of applied potential in an appropriate electrolyte (e.g. storage pond water). A characteristic rise in current density may indicate the corrosion behaviour of the sample which is correlated to the material’s susceptibility under these conditions.

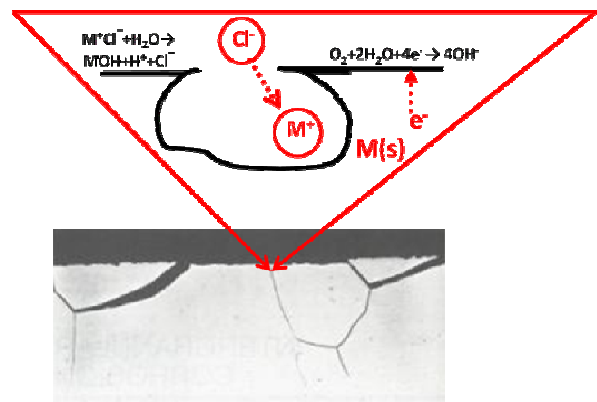
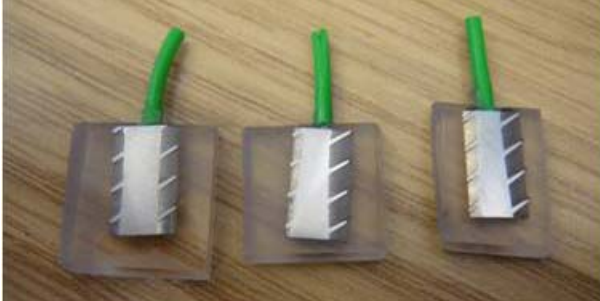


Figure 4 Corrosion processes leading to stress corrosion cracking

**EXPERIMENTAL**

As-received AGR fuel cladding tubes sourced from Sellafield Limited were cut into 10x5 mm sections and solution-annealed at 1050°C for 1 hour followed by water quench. Batches of these sections were then heat treated at 400, 500, 600, 700 and 800 °C, each at residence times of 24, 48, 96 and 192 h, respectively, and furnace-cooled.



**Figure 5** Working electrodes prepared for electrochemical analysis (anodic polarization method)

For each treatment, electrodes are individually prepared by making an electrical connection to the back of the sample which is then mounted in epoxy-resin and subsequently polishing to a 1 µm using diamond abrasive, shown in Figure 5. These electrodes become the working electrode component of a three-electrode cell that employs a silver-silver chloride (Ag|AgCl) reference electrode in a Luggin Capillary and a Pt counter electrode. The whole assembly is enclosed in a Faraday cage to minimize external electrical noise. In addition, separate sets of heat treated samples are reserved for Scanning Electron Microscope (SEM, JOEL5610) and Transmission Electron Microscope (TEM, JOEL FX2000) analysis. Samples for SEM analysis were etched electrolytically at 6.0 V for 10 s in a saturated oxalic acid solution whereas samples for TEM analysis were obtained using a focused ion beam instrument (FIB, FEI Company) to prepare electron transparent cross-sections.

**RESULTS**

Figure 6 is a scanning electron micrograph showing the general microstructure of an as-received AGR fuel cladding.

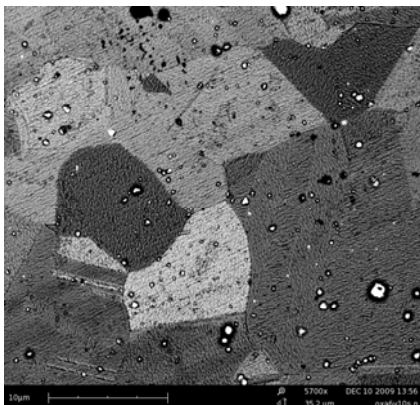


**Figure 6** Backscattered electron Scanning Electron Micrograph of as-received AGR Fuel Cladding

Austenitic grains approximately 10 µm long and wide were revealed with chemical composition (at%) determined as 21.7±0.2, 54.1±0.1, and 24.2±0.2 for Cr, Fe, and Ni, respectively. There were no significant differences in compositions at the grain boundaries. A substantial level of precipitation (scattered white spots) was observed throughout, determined to be from niobium-rich carbide (NbC) precipitates at concentrations (at%) of 71.1±14.4, 3.7±3.3, and 20.9±7.7 for C, Fe and Nb, respectively.

Figure 7 shows a transmission electron micrograph of a 400°C 96 h heat-treated AGR fuel cladding and Table 1 indicates its measured composition at the grains (area I, III, V and VII) and grain boundaries (area II, IV, VI, IX). On average, concentrations of solute Cr, Fe and Ni at the grain boundaries were decreased by 34.2 %, 36.2 %, and 36.3 %, respectively.

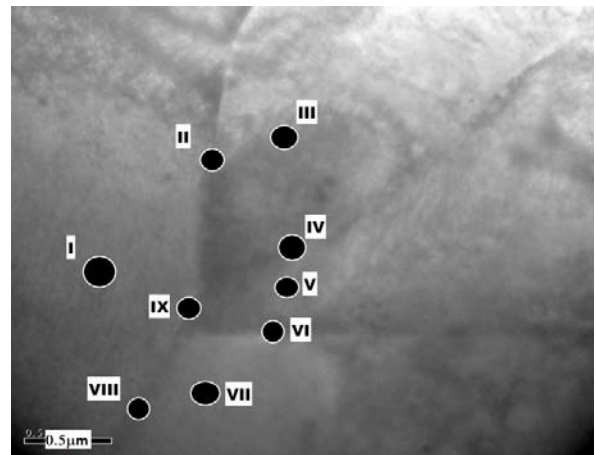


**Figure 7** Bright-field transmission electron micrograph of a 400°C 96 h heat-treated AGR fuel cladding

**Table 1** Energy Dispersive X-ray (EDX) analysis of a 400°C 96 h heat-treated AGR fuel cladding (at%)

Spectrum	C	Si	Cr	FE	Ni	Nb
Grains	38.9±4.6	2.3±0.2	13.2±1.5	31.5±2.1	13.7±1.1	0.4±0.4
Grain Boundaries	60.6±3.5	1.8±0.2	8.7±0.7	20.1±1.9	8.7±0.9	0.1±0.2
% difference	-55.8	23.9	34.2	36.2	36.3	70.6

Figure 8, which shows the polarization curves of the as-received and 400°C 24h heat-treated AGR fuel cladding in a 0.01M NaCl, indicates that the as-received material remains passive for applied potentials up to ~1.5V at approximately the oxygen evolution region but the sensitized material, in contrast, exhibits corrosion at ~0.1V and gradually peaks at ~1.0 V. The measured current is an indication of decreased corrosion resistance due to dissolution along the grain boundary.

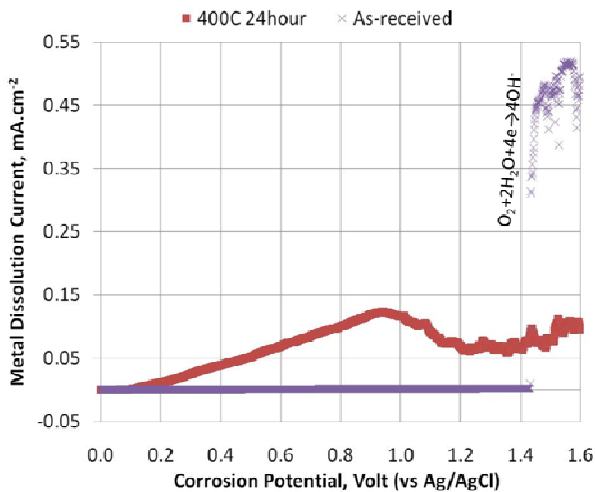


**Figure 8** Polarization curve of as-received and 400°C 24h heat treated AGR fuel cladding in 0.01M of NaCl

## CONCLUSION

Concern about spent AGR fuel cladding corrosion during prolonged storage in a demineralised-water cooling pond prior to reprocessing has prompted an understanding of the effect of trace chloride environments to sensitisation. Representative samples of sensitisation consistence for non-cave experiments have been produced via heat treatment. Discrete levels of grain boundary chromium depletion on the order of 36 at % were produced in a controllable and predictable manner. To date, a thermal treatment of 400°C 96 hours was able to produce in the previously homogeneous as-received AGR fuel cladding a 34.2 at%, 36.2 at% and 36.3 at% reduction in grain boundary concentration of solute Fe, Cr and Ni, respectively. Polarisation data indicate a decrease in corrosion resistance with breakdown potentials as low as 0.1 V (Ag|AgCl) in 0.01M of NaCl.

## ACKNOWLEDGEMENTS

The authors thank Dr. Paul Standring of Sellafield Ltd for providing samples and knowledge support and the EPSRC DIAMOND Consortium for financial support.

## REFERENCES

1. Norris, D. I. R.; Baker, C.; Taylor, C.; Titchmarsh, J. M. In *Radiation-Induced Segregation in 20Cr/25Ni/Nb Stainless Steel*, Effects of Radiation on Materials: 15th International Symposium, Philadelphia, Philadelphia, 1992; pp 603-620.
2. Waddington, J. S.; Jones, R. B. In *Properties of Stainless Steel Cladding For Use in Advanced Gas-Cooled Reactors*, Physical Metallurgy of Reactor Fuel Elements, Berkeley Nuclear Laboratories, Gloucestershire, Harris, J. E.; Skyes, E. C., Eds. The Metals Society: Berkeley Nuclear Laboratories, Gloucestershire, 1973.

3. Okada, O.; Nakata, K.; Kasahara, S., Effects of thermal sensitization on radiation-induced segregation in type 304 stainless steel irradiated with He-ions. *Journal of Nuclear Materials* **1999**, 265 (3), 232-239.
4. Ashworth, M. A.; Norris, D. I. R.; Jones, I. P., Radiation-Induced Segregation in Fe-20Cr-25Ni-Nb Based Austenitic Stainless Steels. *Journal of Nuclear Materials* **1992**, 189 (3), 289-302.
5. Stobbs, J. J.; Swallow, A. J., Effects of Radiation on Metallic Corrosion. *Metallurgical Review* **1962**, 7 (25).
6. Simonen, E. P.; Bruemmer, S. M., Radiation effects on environmental cracking of stainless steels. *Jom-Journal of the Minerals Metals & Materials Society* **1998**, 50 (12), 52-55.
7. Marwick, A. D., Segregation in Irradiated Alloys - Inverse Kirkendall Effect and Effect of Constitution on Void Swelling. *Journal of Physics F-Metal Physics* **1978**, 8 (9), 1849-1861.
8. Sourmail, T.; Too, C. H.; Bhadeshia, H., Sensitisation and evolution of chromium-depleted zones in Fe-Cr-Ni-C systems. *Isij International* **2003**, 43 (11), 1814-1820.
9. Powell, D. J.; Pilkington, R.; Miller, D. A., The Precipitation Characteristics of 20Cr/25Ni/Nb Stabilised Stainless Steel. *Acta Metallurgica* **1988**, 36 (3), 713-724.
10. Evans, H. E.; Lobb, R. C., Conditions for the Initiation of Oxide Scale Cracking and Spallation. *Corrosion Science* **1984**, 24 (3), 209-222.
11. Evans, H. E.; Lobb, R. C., The Influence on Oxide Spallation of Annealing Periods During a Cooling Cycle. *Corrosion Science* **1993**, 35 (5-8), 999-1005.
12. Lobb, R. C.; Evans, H. E. In *The High-Temperature Oxidation of AGR Fuel Cladding*, Materials for Nuclear Reactor Core Applications, Bristol, British Nuclear Energy Society, London: Bristol, 1987.
13. Sedriks, A. J., *Corrosion of stainless steels*. 2nd ed.; John Wiley: New York ; Chichester, 1996.
14. Szklarska-Smialowska, Z., *Pitting corrosion of metals*. National Association of Corrosion Engineers: Houston, Tex., 1986.
15. Moayed, M. H.; Newman, R. C., Deterioration in critical pitting temperature of 904L stainless steel by addition of sulfate ions. *Corrosion Science* **2006**, 48 (11), 3513-3530.
16. Marsh, G. P.; Taylor, K. J.; Bryan, G.; Worthington, S. E., The Influence of Radiation on the Corrosion of Stainless Steel. *Corrosion Science* **1986**, 26 (11), 971-982.